

EFFICIENT SET-THEORETIC ALGORITHMS FOR COMPUTING HIGH-ORDER FORMAN-RICCI CURVATURE ON ABSTRACT SIMPLICIAL COMPLEXES*

DANILLO BARROS DE SOUZA[†], JONATAS T. S. DA CUNHA[‡], FERNANDO A. N. SANTOS[§], JÜRGEN JOST[¶], AND SERAFIM RODRIGUES^{||}

Abstract. Forman-Ricci curvature (FRC) has become a potent and powerful for analysing empirical networks, as the distribution of the curvature values can identify some structural information that is not readily detected by other schemes. For a graph, it is easy to compute, but it is not sensitive to higher-order structural information. That issue can be handled by going to the clique complex of the graph, and in fact, such complexes also emerge as Vietoris-Rips complexes in Topological Data Analysis. But then, with standard methods, it becomes much more computationally expensive. In this paper, we therefore develop a novel set-theoretic formulation for computing such high-order FRC in complex networks. We provide a pseudo-code, a software implementation coined FastForman, as well as a benchmark comparison with alternative implementations. Crucially, our representation theory reveals previous computational bottlenecks and also accelerates the computation of FRC.

Key words. Forman-Ricci curvature, discrete geometry, set theory, optimization, complex systems, higher-order networks, data science.

AMS subject classifications. 05C85, 52C99, 90C35, 62R40, 68T09.

1. Introduction. Network analysis is one of the success stories of complex systems research. The basic is simple, to represent the network as a graph whose mathematical features can then be studied. Beyond the determination of clusters or the identification of particularly important vertices or edges, also certain statistical features can reveal valuable structural information. Among those, the so-called discrete Ricci curvatures (a name derived from their conceptual origin in Riemannian geometry) are particularly useful. And among those curvatures, the Forman Ricci curvature (FRC) is particularly easy to compute. But this comes at the expense of ignoring valuable information that is contained in higher-order relations between the vertices. To uncover such information, it is necessary to go to simplicial complexes, in the case at hand the clique complex of the graph. The topological aspects of such higher-order information are evaluated in Topological Data Analysis (TDA). There, with a scale parameter r , one constructs a graph by connecting pairs of data points whose distance is $\leq r$, and one then computes the homology, and in particular, the Betti numbers,

* Submitted to the editors January 11, 2024.

Funding: This research is supported by the Basque Government through the BERC 2022-2025 program and by the Ministry of Science and Innovation: BCAM Severo Ochoa accreditation CEX2021-001142-S / MICIN / AEI / 10.13039/501100011033. Moreover, this research is financially supported by the IKUR Strategy under the collaboration agreement between the Ikerbasque Foundation and BCAM on behalf of the Department of Education of the Basque Government

[†]Basque Center for Applied Mathematics (danillo.dbs16@gmail.com, dbarros@bcamath.org, <http://www.bcamath.org/en/people/dbarros>).

[‡]Universidade Federal de Pernambuco, Recife, Brazil, (jteodomirosc@gmail.com, jonatas.teodomiro@ufpe.br)

[§]Dutch Institute for Emergent Phenomena (DIEP), Institute for Advanced Studies, University of Amsterdam, Oude Turfmarkt 147, 1012 GC, Amsterdam, The Netherlands, and Korteweg de Vries Institute for Mathematics, University of Amsterdam, Science Park 105-107, 1098 XG Amsterdam, the Netherlands (f.a.nobregasantos@uva.nl)

[¶]Max Planck Institute for Mathematics in the Sciences, Leipzig, and Center for Scalable Data Analytics and Artificial Intelligence, Leipzig University, Germany, and Santa Fe Institute, New Mexico, USA (jost@mis.mpg.de)

^{||}Basque Center for Applied Mathematics, Bilbao, Spain (srodrigues@bcamath.org)

of the resulting clique complex, called the Vietoris-Rips complex, as depending on r . This by now is a well-established method. But in line with the preceding, we want to extract geometric information, and as suggested, this should be done by the augmented FRC of such a complex. Now, these clique or Vietoris-Rips complexes are not arbitrary simplicial complexes but enjoy the special property that every simplex is automatically filled as soon as all its edges, that is, its 1-skeleton are present. However, while the FRC of a graph is very easy to compute, this is no longer so for the augmented FRC of a simplicial complex, at least with standard methods. Therefore, in this paper, we provide a systematic mathematical approach within which the FRC of such a Vietoris-Rips type complex can be easily and quickly computed. As the name indicates, FRC was originally introduced by Forman [12]. It was inspired by Bochner's formula for Ricci tensors in Riemannian manifolds [1]. [12] provides a formula for FRC of a simplicial complex. The graph version has already found a wide range of applications. For instance, it has been applied in cancer diagnostics [20], detecting anomalies on brain networks [3], detection of dynamic changes on data sets [25], detection of stock market fragility [21] and to infer pandemic states [6]. But in those and other cases, usually only the FRC of a graph was computed. To reveal the full power of the scheme, and to systematically compare the results with those obtained by TDA, we need to compute the FRC of such simplicial complexes. But in general, the time and memory complexity of computing higher-order dimensional information from complex networks is prohibitively expensive, which often limits applications. For example, the time for computing all cliques in a graph has exponential-time complexity [7, 11, 18]. Also, the Betti number computation required for TDA is an NP-hard problem [9], due to the matrix construction of boundary operators. Indeed, Betti number computation increases with the number of cliques and, consequently, requires memory-efficient algorithms. Likewise, the lack of efficient algorithms for computing generalized geometric structures has limited the use of high-order Forman-Ricci curvature (FRC) for complex networks. Set-theoretic approaches [10, 14, 17, 28] may offer a solution to this problem, and this is the approach of the present paper. To implement and apply this, we make an important observation that when the complex is of Vietoris-Rips type, that is, all simplices are filled when their 1-skeleton is present, this leads to considerable computational simplifications. And, incidentally, this is also a reason why TDA is such a powerful scheme in applications. Therefore, our assumption seems natural, and we then want to build an algorithm upon it. To this end, we developed a set-theoretic representation theory for higher-order network structures based on node neighbourhoods to give an alternative (and optimal) definition for FRC in terms of the classic node neighbourhood of a graph. This leads us to a representation theory that reveals previous computational bottlenecks and enables us to develop an efficient algorithm that markedly accelerates the computation of FRC in higher-order networks. We have implemented our algorithm - FastForman (see in [5]) - and benchmarked it with other implementations, namely GeneralisedFormanRicci [27] and HodgeLaplacians [23]. We found that our implementation boosted time processing and drastically reduced memory consumption during the process of computing FRC for low and high-dimensional network structures. These results reinforce our beliefs in the power of set-theoretic approaches to improve the efficiency of algorithm implementations for high-order geometric approaches to big data sets.

2. Network and higher-order network fundamentals. An *undirected simple graph* (or network) $G = (V, E)$ is defined by a finite set of nodes V and a *set of edges* $E = \{(x, y) \mid x, y \in V, x \neq y\}$. **Example 6.1** depicts the definition of a simple

graph.

Let $x, y \in V$. We say that y is a *neighbour* of x if the edge $(x, y) \in E$. The *neighbourhood* of the node x is defined by a set of nodes that are connected to x via an edge in E , and we denote by π_x . Formally,

$$(2.1) \quad \pi_x = \{y \in V \mid (x, y) \in E\},$$

A simple example is shown in [Example 6.2](#). We will define the *Graph neighbourhood* as the sequence of node neighbourhoods of a graph G . Formally,

$$(2.2) \quad \text{Neigh}(G) = (\pi_x \mid x \in V)$$

An easy and efficient implementation for finding node neighbourhood is provided in [Algorithm 2.1](#).

Algorithm 2.1 Compute Graph Neighborhood: Neigh(G)

```

Input:  $G = (V, E)$ 
 $\pi_x = \emptyset, \forall x \in V$ 
for  $e = (x, y) \in E$  do
   $\pi_x := \pi_x \cup \{y\}$ 
   $\pi_y := \pi_y \cup \{x\}$ 
end for
return  $\pi_x$  for all  $x \in V$ 

```

2.1. Abstract simplicial complex. The concepts of this section are as defined from [8,29,30]. Let C be a set together with a collection \mathcal{S} . We say that C is an abstract simplicial complex if the following conditions are satisfied:

1. For each $v \in C$, $\{v\} \in \mathcal{S}$;
2. If $\gamma \subseteq \alpha$ and $\alpha \in \mathcal{S}$, then $\gamma \in \mathcal{S}$.

We say that α are *d-cells* (or $(d+1)$ -cliques) if $|\alpha| = d+1$. When $\gamma \subseteq \alpha$, we say that γ is a *face* of α , or alternatively, α is a *coface* of γ . In our approach, in the special cases where $|\alpha|=|\gamma|+1$, we will denote $\gamma < \alpha$, or alternatively, $\alpha > \gamma$. We denote the set of all *d-cells* by C_d , and we can clearly reconstruct C by taking $C = \bigcup_d C_d$. Let $G = (V, E)$

be a simple undirected graph. The collection \mathcal{C} of all subsets of $\{x_0, x_1, \dots, x_d\} \subseteq V$ such that the vertices span a cell of C is called a *vertex scheme* of C . Clearly, \mathcal{C} is a simplicial complex and can be identified to C via isomorphism [16]. This result allows us to identify a cell $\alpha \in C_d$ with the a subset $\{x_0, \dots, x_d\} \subseteq V$. Also, any combinations of subsets with size k span a $(k-1)$ -cell in C_{k-1} , for $k \in \{1, \dots, d\}$. We refer the reader to [Figure 1](#) and accompanying [Example 6.3](#) for a graphic exposition of the concepts of simplicial complex and d-cells. Analogous to definition (2.1), we define the *node neighborhood of a d-cell* α (or the *neighbouring of nodes of a d-cell*) as follows:

$$(2.3) \quad \pi_\alpha = \bigcap_{x \in \alpha} \pi_x.$$

An application of this formulation can be accessed in [Example 6.4](#). Note that for $d = 1$ in equation (2.3) we reach back to the classical formula of the neighbourhood of a node described by equation (2.1).

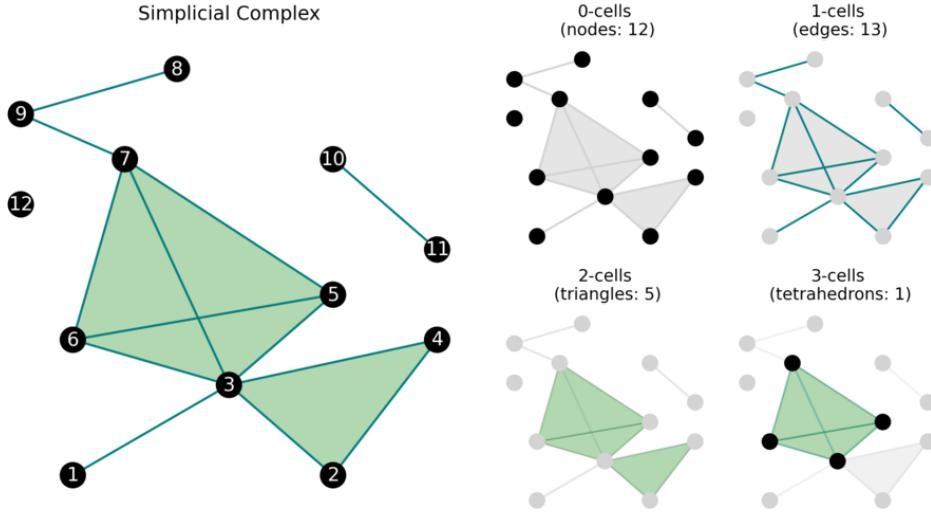


FIG. 1. *Example of a simplicial complex and its d -cells for $d \in \{0, 1, 2, 3\}$. In this example, we have 12 nodes (0-cells), 13 edges (1-cells), 5 triangles (2-cells) and 1 tetrahedron (3-cells).*

3. High-order Forman-Ricci curvature. Let $G = (V, E)$ a graph and $d \in \mathbb{N} \cup \{0\}$. Let $\alpha \in C_d$. We define the *boundary* of α by $\partial(\alpha) = \{\gamma \in C_{d-1}, \gamma < \alpha\}$, for $d > 0$ and $\partial(\alpha) = \emptyset$ for $d = 0$. Alternatively, we can define $\partial(\alpha) = \{\{x_0, \dots, \hat{x}_i, \dots, x_d\}, x_i \in \alpha\} = \{\gamma \subset \alpha, |\gamma| = d\}$, where \hat{x}_i denotes the removal of element x_i . Note that $\partial(\alpha)$ has exactly $\binom{d+1}{d} = d + 1$ elements. In [Example 6.5](#) the concept of cell boundary is elucidated. We say that $\alpha_1, \alpha_2 \in C_d$ are *neighbours* if at least one of the following *cell neighborhood conditions* is reached:

1. There exists a $(d - 1)$ -cell γ such that $\gamma < \alpha_1, \alpha_2$;
2. There exists a $(d + 1)$ -cell β such that $\alpha_1, \alpha_2 < \beta$.

We say that α_1 and α_2 are *parallel neighbours* if conditions 1. are reached, but not 2. and we denote the parallelism by $\alpha_1 // \alpha_2$. In case of both conditions, 1. and 2. are satisfied, α_1 and α_2 are said *transverse neighbours*. [Example 6.6](#) elucidates the concept of cell neighbourhood. Let $\alpha \in C_d$. We denote the set of all neighbours of a cell α by N_α . The sets of parallel and transverse neighbours of α will be denoted by P_α and T_α , respectively. We will also denote by H_α as the set of all $(d + 1)$ -cells that have α in its boundary, i.e, all $\beta \in C_{d+1}$, such that $\beta > \alpha$. From conditions 1. and 2., it is clear that these sets are disjoint, and we can also write

$$(3.1) \quad N_\alpha = P_\alpha \sqcup T_\alpha,$$

for all $d \geq 1$ and all $\alpha \in C_d$.

Remark 3.1. We emphasize that the concepts of node neighbourhood of a cell and cell neighbourhood are strongly related, however, they describe completely different objects. While the node neighbourhood of a cell describes the set of nodes that has a common intersection with all nodes of the cell in question (as defined in [\(2.1\)](#) and [\(2.3\)](#)), the cell neighbourhood are all cells in the simplicial complex that reach at least one of the cell neighbourhood conditions. A comparison between [Example 6.2](#) and [Example 6.4](#) can elucidate the explanation of this difference. The link between the

two concepts occurs from the fact that the neighbours of a cell α can be described in terms of the node neighbourhood of the sub-cells in its boundary, which will be clarified along the construction of our set-theoretic definitions.

The d -th *Forman-Ricci curvature* (FRC) is then given as follows [22, 26]:

$$(3.2) \quad \begin{aligned} F_d(\alpha) = & |\{\beta \in C_{d+1}, \beta > \alpha\}| \\ & + |\{\gamma \in C_{d-1}, \gamma < \alpha\}| \\ & - |\{\alpha' \in C_d, \alpha' // \alpha\}|, \end{aligned}$$

where $|\cdot|$ is the number of elements in the set (i.e. cardinality). Alternatively, it can be formulated as follows:

$$(3.3) \quad F_d(\alpha) = |H_\alpha| + (d+1) - |P_\alpha|.$$

Note, for example, when $d = 1$, we have recovered the classic FRC of an edge $e \in E = C_1$ as

$$(3.4) \quad F(e) = |\{t \in C_2, t > e\}| + 2 - |\{e' \in E, e' // e\}|,$$

where t denotes a triangle (2-cell). The d -th FRC of a non-empty C_d complex is given by the average of the Forman-Ricci curvatures by cell, *i.e.*,

$$(3.5) \quad F_d(C) = \frac{1}{|C_d|} \sum_{\alpha \in C_d} F_d(\alpha).$$

The computation of FRC for dimensions $d = 1$ and $d = 2$ can be clarified in [Example 6.8](#).

4. Results. Subsequently, we propose our set-theoretic representation theory for high-order network cells and FRC and develop the associated efficient algorithm computing high-order FRC in complex networks.

4.1. Set-theoretic representation of Forman-Ricci curvature. The set of neighbours of α can be redefined in terms of the node neighbourhood as follows (see [Theorem 7.5](#)):

$$(4.1) \quad N_\alpha = \bigsqcup_{\gamma \in \partial(\alpha)} \bigcup_{\substack{x \in \pi_\gamma \neq \emptyset \\ x \notin \alpha}} \{\gamma \cup \{x\}\},$$

where the \bigsqcup operation represents the disjoint union of sets. The [Theorem 7.4](#) also characterizes the neighbours of a d -cell by finding cells that reach the cell neighbouring condition 1., which means that it is sufficient for two d -cells to have a common boundary to be neighbours. The transverse neighbours of α can also be characterized (see [Theorem 7.7](#)), which lead as to the formula

$$(4.2) \quad T_\alpha = \bigsqcup_{\gamma \in \partial(\alpha)} \bigcup_{\substack{x \in \pi_\gamma \neq \emptyset \\ x \in \pi_\alpha \neq \emptyset \\ x \notin \alpha}} \{\gamma \cup \{x\}\}.$$

From (4.2) and (3.1), we derive the set of parallel cells from a complementary set of transverse cells,

$$(4.3) \quad P_\alpha = \bigsqcup_{\gamma \in \partial(\alpha)} \bigcup_{\substack{x \in \pi_\gamma \neq \emptyset \\ x \notin \pi_\alpha \neq \emptyset \\ x \notin \alpha}} \{\gamma \cup \{x\}\}.$$

In practical terms, equations (4.2) and (4.3) suggest that the transverse and parallel cells can be obtained from (4.1) by deciding if each neighbouring cell of α is contained in a $(d+1)$ -cell or not. The details are shown in [Theorem 7.8](#). Also, from [Theorem 7.10](#),

$$(4.4) \quad |T_\alpha| = (d+1) |H_\alpha|,$$

which together with (3.3) provides

$$(4.5) \quad F(\alpha) = \frac{1}{(d+1)} |T_\alpha| + (d+1) - |P_\alpha|,$$

which after expansion provides

$$(4.6) \quad F(\alpha) = \frac{1}{(d+1)} \sum_{\gamma \in \partial(\alpha)} |\pi_\alpha \cap \pi_\gamma - \alpha| + (d+1) - \sum_{\gamma \in \partial(\gamma)} |\pi_\gamma - \pi_\alpha - \alpha|.$$

Moreover, we can express the number of cells of dimension $d+1$ containing α (see proof in [Theorem 7.9](#)) as

$$(4.7) \quad H_\alpha = \bigcup_{x \in \pi_\alpha \neq \emptyset} \{\alpha \cup \{x\}\}.$$

It follows from equations (3.1), (4.1) and (4.2) that

$$(4.8) \quad F_d(\alpha) = |\pi_\alpha| + (d+1) - \sum_{\gamma \in \partial(\gamma)} |\pi_\gamma - \pi_\alpha - \alpha|.$$

Equation (4.8) provides a direct computation of FRC from the parallel cells. However, an alternative equation can be derived by computing FRC directly from the cell neighbourhood. This is obtained by combining (3.1), (3.3) and (4.4) we have

$$(4.9) \quad F_d(\alpha) = (d+2) |\pi_\alpha| + (d+1) - |N_\alpha|.$$

The expansion of the term $|N_\alpha|$ leads to

$$(4.10) \quad |N_\alpha| = \sum_{\gamma \in \partial(\alpha)} |\pi_\gamma - \alpha| = \sum_{\gamma \in \partial(\alpha)} |\pi_\gamma| - (d+1),$$

which when applied to (4.9) leads us to

$$(4.11) \quad F_d(\alpha) = (d+2) |\pi_\alpha| + 2 \cdot (d+1) - \sum_{\gamma \in \partial(\alpha)} |\pi_\gamma|,$$

Equations (4.6), (4.8) and (4.11) not only establish new formulations for FRC but also crucially enable us to propose novel algorithms to efficiently compute FRC in terms of the local node neighbourhoods of the cells into consideration. We propose [Algorithms 4.1 to 4.3](#) that should be parameterized by the graph $G = (V, E)$, the list of cells (C) , and the maximum cell dimension (d_{\max}) , and it computes FRC up to dimension $d \leq d_{\max}$.

Algorithm 4.1 Compute Forman-Ricci Curvature: Method A

Input: $C, d_{\max} \geq 1$
 $\mathcal{F}_d = \emptyset, \forall d \leq d_{\max}$
Compute Neigh(G) from [Algorithm 2.1](#);
for $\alpha \in C$ **do**
 $d := |\alpha| - 1$
 Compute $F_d(c)$ according to (4.6):
 Compute π_α ;
 for $\gamma \in \partial(\alpha)$ **do**
 set $M := \{v \in V \mid v \in \pi_\gamma, v \notin \alpha\}$, $t := 0, p := 0$;
 for $v \in M$ **do**
 if $v \in \pi_\alpha$ **then**
 $t := t + 1$
 else
 $p := p + 1$
 end if
 end for
 end for
 set $F_d(\alpha) = \frac{1}{(d+1)} \cdot t + (d+1) - p$
 Update $\mathcal{F}_d := \mathcal{F}_d \cup \{F_d(\alpha)\}$
end for
return $\mathcal{F} = \bigcup_d \{\mathcal{F}_d\}$

Algorithm 4.2 Compute Forman-Ricci Curvature: Method B

Input: $C, d_{\max} \geq 1$
 $\mathcal{F}_d = \emptyset, \forall d \leq d_{\max}$
Compute Neigh(G) from [Algorithm 2.1](#);
for $\alpha \in C$ **do**
 $d := |\alpha| - 1$
 Compute $F_d(c)$ according to (4.8):
 Compute π_α ;
 Set $p := 0$;
 for $\gamma \in \partial(\alpha)$ **do**
 set $M := \{v \in V \mid v \in \pi_\gamma, v \notin \alpha\}$
 for $v \in M$ **do**
 if $v \notin \pi_\alpha$ **then**
 $p := p + 1$
 end if
 end for
 end for
 set $F_d(\alpha) = |\pi_\alpha| + (d+1) - p$
 Update $\mathcal{F}_d := \mathcal{F}_d \cup \{F_d(\alpha)\}$
end for
return $\mathcal{F} = \bigcup_d \{\mathcal{F}_d\}$

Algorithm 4.3 Compute Forman-Ricci Curvature: Method C

```

Input:  $C, d_{\max} \geq 1$ 
 $\mathcal{F}_d = \emptyset, \forall d \leq d_{\max}$ 
Compute Neigh(G) from Algorithm 2.1;
for  $\alpha \in C$  do
   $d := |\alpha| - 1$ 
  Compute  $F_d(\alpha)$  according to (4.11):
  Set  $h := |\pi_\alpha|$  and  $n := 0$ ;
  for  $\gamma \in \partial(\alpha)$  do
    Update  $n := n + |\pi_\gamma|$ ;
    Set  $F_d(\alpha) = (d + 2)h + 2(d + 1) - n$ ;
  end for
  Update  $\mathcal{F}_d := \mathcal{F}_d \cup \{F_d(\alpha)\}$ 
end for
return  $\mathcal{F} = \bigcup_d \{\mathcal{F}_d\}$ 

```

4.2. Computation and Benchmark of Novel Algorithms. To validate our set-theoretic representation of FRC, we developed a Python language version [24] of our pseudo-codes, which we named **FastForman** - Method A, B and C, which uses the formulation (4.6), (4.8) and (4.11), respectively. Furthermore, we run benchmark tests and compared **FastForman**'s execution time and memory usage with the leading software in the literature, namely Python packages **HodgeLaplacians** [23] and **GeneralisedFormanRicci** [27]. The benchmark tests were performed on a Dell laptop model XPS 15-7590, Intel Core i7-9750H CPU 2.60GHz, 32Gb RAM, running Linux Ubuntu operating system version 20.04.4 LTS (Focal Fossa). To carry out the tests, with the help of **NetworkX** package [13], we generated 20 copies of 3-dimensional point cloud data from random geometric networks [19] with the parameters $n = 50$ nodes and radius $r \in \{0.1, 0.2, \dots, 1.0\}$ (to access this data we refer the reader to the link [5]). To undertake an unbiased benchmark test, it is first worth noting that the Python package, **GeneralisedFormanRicci**, is limited to computing the FRC for edges and triangles. Therefore, we divided the benchmark tests into two separate groups. The first group aimed at comparing **GeneralisedFormanRicci**, **HodgeLaplacians** and **FastForman** (A, B and C) for $d_{\max} = 2$. The second group focused on comparing **HodgeLaplacians** versus **FastForman** (A, B and C) for $d_{\max} = 5$. To compare the time complexity between all involved software packages, we considered the total execution time from the generation of cells (cliques) to the end computation of FRC. For a fair comparison, we employed the same software package, **Gudhi** [15], to list the cells of the aforementioned generated networks. Due to the separate benchmark groups, we first depict in Figure 3 the average number of cells for $d_{\max} \in \{2, 5\}$ contained within the aforementioned generated networks. In Figure 4 we benchmark the average of the total processing time and average memory peak usage for computing the FRC over the generated random networks. We also compare the results with the time and memory consumption of listing the set of cells via the **Gudhi** package (light blue curves in the figure). We subsequently discuss the merits and limitations of each software package for computing FRC.

GeneralisedFormanRicci: Due to computational limitations with memory management, we could not compute FRC for radius values higher than $r = 0.7$ via **GeneralisedFormanRicci**. Despite **GeneralisedFormanRicci** being limited to lower

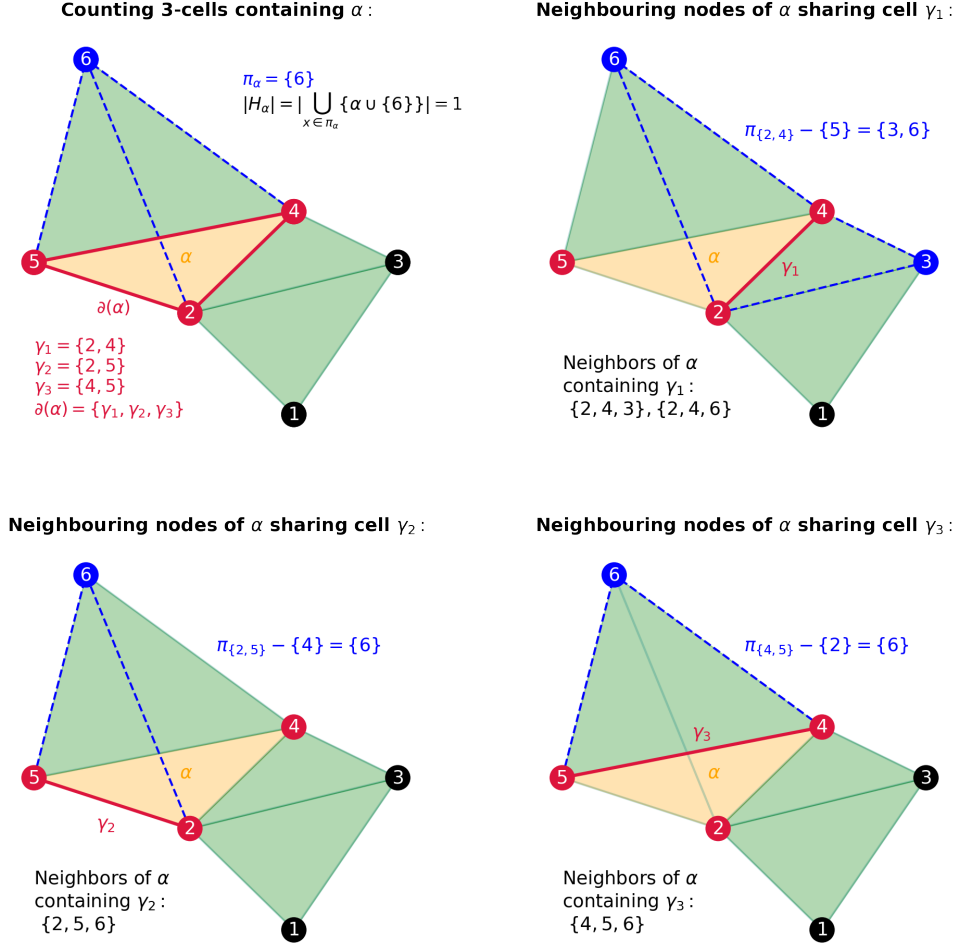


FIG. 2. Example of how the algorithm detects cell neighbours from node neighbourhood for 2-cells (triangles). The 2-cell α is enhanced in orange, whilst its boundary is drawn in red. According to the algorithm, the number of 3-cells containing α in its boundary ($|H_\alpha|$) coincides with the number of common neighbours of the nodes in α ($|\pi_\alpha|$). Also, the number of neighbours per boundary is counted by the size of intersections of node neighbourhoods in the boundary. In this example, $F_2(\alpha) = 4 \cdot |\{6\}| + 3 - (|\{3, 6\}| + |\{6\}| + |\{6\}|) = 3$. The same output is reached by using (3.2): $F_2(\alpha) = 1 + 3 - 1 = 3$.

dimensional computations, the time consumption was the highest, exceeding the **Hodgelaplacians** and **FastForman** implementations. Moreover, it displays a high variance of time and memory consumption particularly for dense networks, which might be associated with its limitations in computing FRC up to 2-dimensional cells (compare **Figures 3** and **4**). The limitation to point cloud data sets is also a drawback of the algorithm since it restricts one from selecting a subset of cells over which one may compute FRC.

Hodgelaplacians: The time processing is comparable with the performance results of **FastForman** for low-dimensional cells and low connectivity values. However, the computational efficiency decreases for high-order cells and larger radii and thus

its performance falls behind in comparison to **FastForman**. Furthermore, the time and memory processing variance increase significantly with respect to the network complexity (*ie.*, size, number of higher-order cells and density). This fact might be explained by the computation of FRC via Bochner’s discrete formula, which uses Hodge Laplacian and Bochner Laplacian matrix operators [2, 4, 26]. This demands memory for storing the matrices and time to both generate the matrices and compute FRC. It is worth emphasising that the Hodge Laplacian matrix for the highest cell dimension is simply the d_{\max} -th boundary operator, which in computational terms, induces a miscalculation on FRC for this dimension. Thus, for the correct computation for all cells, the entire simplicial complex should be provided, which impacts directly on the computational complexity. One way to improve efficiency and avoid miscalculation would be to include information of $(d_{\max} + 1)$ -cells so the correct computation up to d_{\max} can be computed correctly. A detailed report of this special case is included in the link [5], where we provide an example of the miscalculation.

FastForman: Our implementations had equivalent performance and superseded existing FRC software packages benchmarked in our tests. The key to this performance is that our set-theoretic formulation leads us to algorithms that only require the use of local node neighbourhood information for computing the FRC by cell, which, as a consequence, reduces the complexity of computing FRC. Noteworthy, there is no requirement for specifically computing and storing neighbouring cells, hence this explains its low memory usage and fast computation. Moreover, **FastForman** implementations are versatile in the sense that they do not make mandatory the inclusion of the global information of an entire simplicial complex. In other words, the FRC computation is flexible, in a way that it can be computed for subsets of cells within a given simplicial complex. The limiting factors are twofold: Firstly, the complexity of the algorithms is dependent upon how cells are computed, which is generically an NP-problem and herein we employed the **Gudhi** algorithm. Secondly, the algorithm’s complexity is associated with node neighbourhood computation, as given by **Algorithm 2.1**, which has a time complexity of $\mathcal{O}(|E|)$ since it iterates over edges. Indeed, **FastForman**’s implementation processing time increases in accordance with the time required for finding cells; see **Figures 3** and **4**. To be more precise, the space complexity is, in the worse case (when the graph is complete), $\mathcal{O}(C(d_{\max}) + |V|^2)$, where $C(d_{\max})$ is the space complexity for the finding cliques algorithm (up to dimension d_{\max}) and $|V|^2$ is the space complexity for storing the neighbourhood of nodes, in the worse scenario. The time complexity is $\mathcal{O}(\sum_{d=1}^{d_{\max}} |C_d| \cdot (d + 1) \cdot |V|^{(d+1)})$, where $(d + 1)$ is the time complexity for iterating the boundary of a d -cell and $|V|^{(d+1)}$ is the order complexity for computing set intersection of $(d + 1)$ node neighbourhoods (taking into account that we can compute set intersection in $\mathcal{O}(\sum_{x \in \alpha} |\pi_x|)$ time). As an application, we showcase our optimal performance in random graphs, aiming to extend the results on geometry detection from the work in [26]. From **Theorem 7.11**, we are able to compare the exact range of values reached by FRC as a function of the number of nodes and the maximum cell dimensions. Moreover, we show we can easily compute the frequency (or distribution) of FRC values in function of the dimension of the cells and compare them across different geometric graphs. To this end, we generated the expected frequency of FRC values for 1000 random graphs in each of the following cases: Erdős-Renyi, 2D Random Geometric, Barabási-Albert and Watts-Strogatz model (with edge randomization parameter $p = 0.25$). All graphs were set up with $n = 50$ nodes and an approximate density of 0.5. We computed the FRC distributions for $d \in \{1, 2, 3, 4\}$, which can be seen in **Figure 5**. Observe that

the standard deviation of the FRC values decreases as the FRC dimension increases. Also, the Watts Strogatz curve becomes less distinguishable from Erdős-Renyi, which may indicate that the random features of Watts Strogatz can be detected only via higher-order analysis. In general, all FRC could be used for geometry detection.

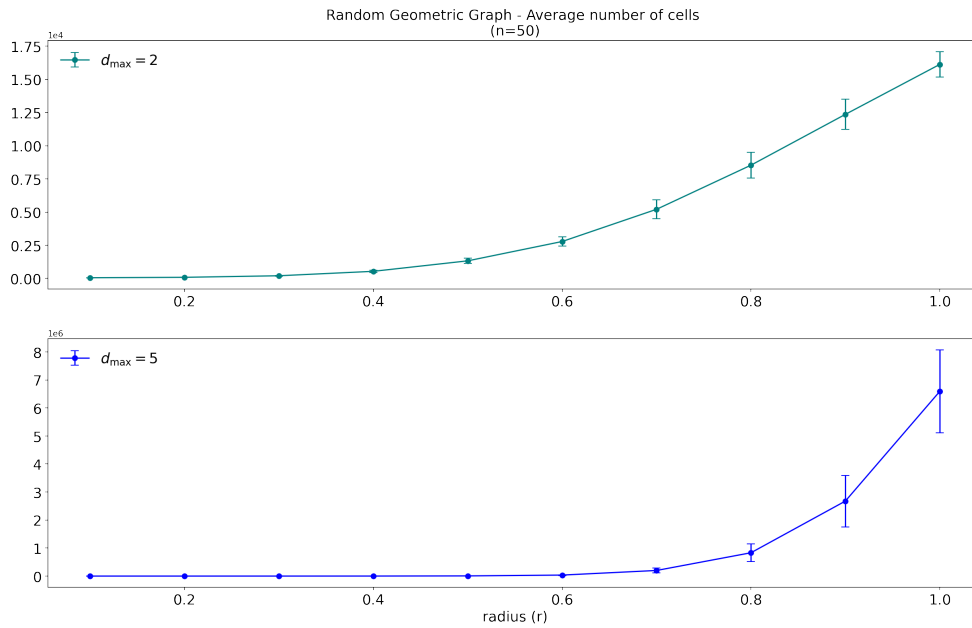


FIG. 3. Average number of cliques for the set of 50 point cloud data, and $d_{\max} \in \{2, 5\}$.

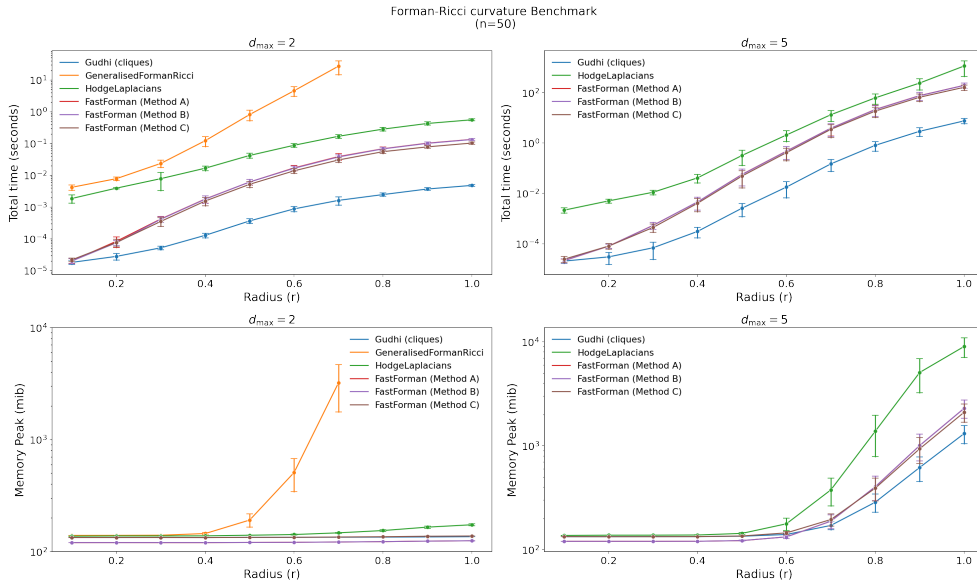


FIG. 4. Benchmark for computing Forman-Ricci curvature by using HodgeLaplacians, GeneralisedFormanRicci and FastForman With methods A, B and C, in comparison with the cells computation by using the Gudhi algorithm, for $n = 50$ and $d_{\max} \in \{2, 5\}$. We display the result in a log scale to clarify the analysis.

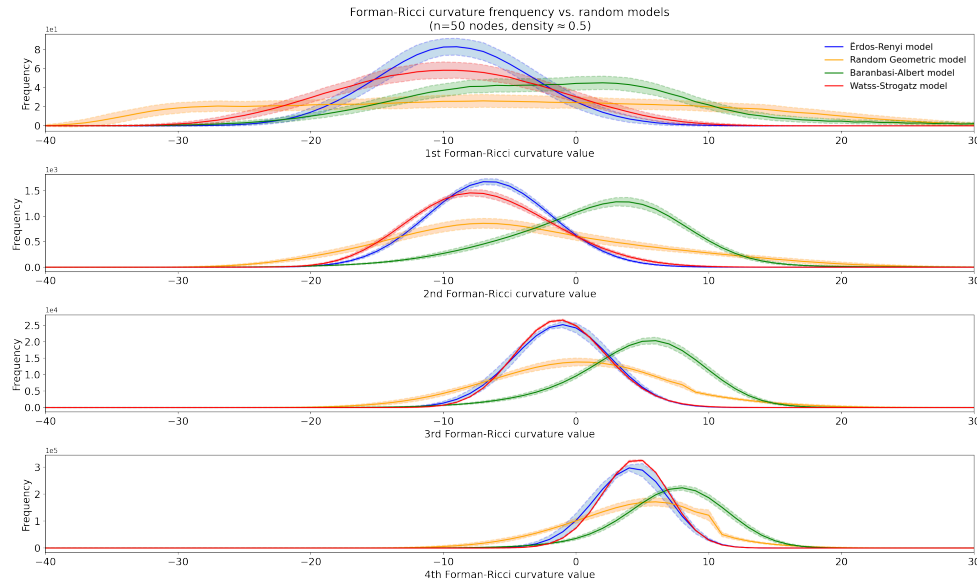


FIG. 5. Comparison of FRC for higher order dimensions between different random graph models.

5. Conclusion. We proposed novel set theoretical formulations for high-order Forman-Ricci curvature (FRC) and this led us to the implementations of new al-

gorithms, which we coined **FastForman** (Method A, B and C). Central to our set-theoretic representation theory for high-order network cells and FRC computation is the fact we managed to redefine parallelism and transversality of neighbouring cells. This enabled us to formulate FRC computation in terms of the neighbours of nodes in a network. As a consequence, we managed to computationally tame some of the combinatorial complexities intrinsic to high-order networks. We validated **FastForman** algorithms via benchmark tests on random higher-order geometric graphs and compared them with leading softwares, namely, **Hodgelaplacians** and **GeneralisedFormanRicci**. To ensure a fair comparison, we implemented **FastForman** with Python language since **Hodgelaplacians** and **GeneralisedFormanRicci** are also implemented in Phyton. We also took into consideration the intrinsic limitations of **Hodgelaplacians** and **GeneralisedFormanRicci**, such as the maximum number of cell dimensions tolerated by these algorithms. Our benchmark tests established that **FastForman** implementations are more efficient in time and memory complexity. In conclusion, despite the constraints of cell search NP algorithms and the combinatorial explosion of high-order network structures, our findings facilitate the computation of higher-order geometric invariants in complex networks. We envisage that **FastForman** will open novel research avenues in big data science, particularly through a geometrical point of view.

Acknowledgments. The authors would like to acknowledge Rodrigo A. Moreira at the Basque Center for Applied Mathematics for his critical review. This research is supported by the Basque Government through the BERC 2022-2025 program and by the Ministry of Science and Innovation: BCAM Severo Ochoa accreditation CEX2021-001142-S / MICIN / AEI / 10.13039/501100011033. Moreover, the authors acknowledge the financial support received from the IKUR Strategy under the collaboration agreement between the Ikerbasque Foundation and BCAM on behalf of the Department of Education of the Basque Government. SR further acknowledges the RTI2018-093860-B-C21 funded by (AEI/FEDER, UE) and the acronym “Math-NEURO”.

REFERENCES

- [1] S. BOCHNER, *Vector fields and ricci curvature*, (1946).
- [2] K. BÖRNER, S. SANYAL, A. VESPIGNANI, ET AL., *Network science*, Annu. rev. inf. sci. technol., 41 (2007), pp. 537–607.
- [3] T. CHATTERJEE, R. ALBERT, S. THAPLIYAL, N. AZARHOOSHANG, AND B. DASGUPTA, *Detecting network anomalies using forman-ricci curvature and a case study for human brain networks*, Scientific reports, 11 (2021), p. 8121.
- [4] S. DAKURAH, D. V. ANAND, Z. CHEN, AND M. K. CHUNG, *Modelling cycles in brain networks with the hodge laplacian*, in International Conference on Medical Image Computing and Computer-Assisted Intervention, Springer, 2022, pp. 326–335.
- [5] D. B. DE SOUZA, *Forman-ricci curvature benchmark report*, 2023, <https://www.kaggle.com/datasets/danillosouza2020/forman-ricci-curvature-benchmark-report>.
- [6] D. B. DE SOUZA, J. T. S. DA CUNHA, E. F. DOS SANTOS, J. B. CORREIA, H. P. DA SILVA, J. L. DE LIMA FILHO, J. ALBUQUERQUE, AND F. A. N. SANTOS, *Using discrete ricci curvatures to infer COVID-19 epidemic network fragility and systemic risk*, Journal of Statistical Mechanics: Theory and Experiment, 2021 (2021), p. 053501, <https://doi.org/10.1088/1742-5468/abed4e>, <https://doi.org/10.1088/1742-5468/abed4e>.
- [7] P. D. DIEU ET AL., *Average polynomial time complexity of some np-complete problems*, Theoretical computer science, 46 (1986), pp. 219–237.
- [8] H. EDELSBRUNNER AND J. L. HARER, *Computational topology: an introduction*, American Mathematical Society, 2022.
- [9] H. EDELSBRUNNER AND S. PARSA, *On the computational complexity of betti numbers: reductions*

- from matrix rank, in Proceedings of the twenty-fifth annual ACM-SIAM symposium on discrete algorithms, SIAM, 2014, pp. 152–160.
- [10] H. B. ENDERTON, *Elements of set theory*, Academic press, 1977.
 - [11] M. R. FELLOWS, F. A. ROSAMOND, U. ROTICS, AND S. SZEIDER, *Clique-width is np-complete*, SIAM Journal on Discrete Mathematics, 23 (2009), pp. 909–939.
 - [12] R. FORMAN, *Bochner’s method for cell complexes and combinatorial ricci curvature*, Discrete and Computational Geometry, 29 (2003), pp. 323–374.
 - [13] A. HAGBERG AND D. CONWAY, *Networkx: Network analysis with python*, URL: <https://networkx.github.io>, (2020).
 - [14] T. J. JECH, T. JECH, T. J. JECH, G. B. MATHEMATICIAN, T. J. JECH, AND G.-B. MATHÉMATICIEN, *Set theory*, vol. 14, Springer, 2003.
 - [15] C. MARIA, J.-D. BOISSONNAT, M. GLISSE, AND M. YVINEC, *The gudhi library: Simplicial complexes and persistent homology*, in International congress on mathematical software, Springer, 2014, pp. 167–174.
 - [16] J. R. MUNKRES, *Elements of algebraic topology*, CRC press, 2018.
 - [17] Z. PAWLAK, *Rough set theory and its applications*, Journal of Telecommunications and information technology, (2002), pp. 7–10.
 - [18] R. PEETERS, *The maximum edge biclique problem is np-complete*, Discrete Applied Mathematics, 131 (2003), pp. 651–654.
 - [19] M. PENROSE, *Random geometric graphs*, vol. 5, OUP Oxford, 2003.
 - [20] R. SANDHU, T. GEORGIU, E. REZNIK, L. ZHU, I. KOLESOV, Y. SENBABAAGLU, AND A. TANNENBAUM, *Graph curvature for differentiating cancer networks*, Scientific reports, 5 (2015), p. 12323.
 - [21] R. S. SANDHU, T. T. GEORGIU, AND A. R. TANNENBAUM, *Ricci curvature: An economic indicator for market fragility and systemic risk*, Science advances, 2 (2016), p. e1501495.
 - [22] E. SAUCAN AND M. WEBER, *Forman’s ricci curvature-from networks to hypernetworks*, in International conference on complex networks and their applications, Springer, 2018, pp. 706–717.
 - [23] M. TSITSVERO, *Hodgelaplacians*, 2019, <https://github.com/tsitsvero/hodgelaplacians>.
 - [24] G. VAN ROSSUM AND F. L. DRAKE JR, *Python reference manual*, Centrum voor Wiskunde en Informatica Amsterdam, 1995.
 - [25] M. WEBER, J. JOST, AND E. SAUCAN, *Forman-ricci flow for change detection in large dynamic data sets*, Axioms, 5 (2016), p. 26.
 - [26] M. WEBER, E. SAUCAN, AND J. JOST, *Characterizing complex networks with forman-ricci curvature and associated geometric flows*, Journal of Complex Networks, 5 (2017), pp. 527–550.
 - [27] J. WEE, *Generalisedformanricci*, 2020, <https://github.com/ExpectozJJ/GeneralisedFormanRicci>.
 - [28] H.-J. ZIMMERMANN, *Applications of fuzzy set theory to mathematical programming*, Information sciences, 36 (1985), pp. 29–58.
 - [29] A. ZOMORODIAN, *Fast construction of the vietoris-rips complex*, Computers & Graphics, 34 (2010), pp. 263–271.
 - [30] A. J. ZOMORODIAN, *Topology for computing*, vol. 16, Cambridge university press, 2005.

Supplementary Materials.

6. Examples. In this section, we provide examples of our work.

EXAMPLE 6.1 (Undirected Simple Graph). *In Figure 1, we have a undirected simple graph, $G = (V, E)$, such that $V = \{1, \dots, 12\}$ and*

$$E = \{(1, 3), (2, 3), (2, 4), (3, 4), (3, 5), (3, 6), (3, 7), (5, 6), (5, 7), (6, 7), (7, 9), (8, 9), (10, 11)\}$$

EXAMPLE 6.2 (Neighborhood of a node). *In Figure 1, we have the neighbors of each node in V as described below:*

$$\begin{aligned} \pi_1 &= \{3\}, \\ \pi_2 &= \{3, 4\}, \\ \pi_3 &= \{1, 2, 4, 5, 6, 7\}, \\ \pi_4 &= \{2, 3\}, \\ \pi_5 &= \{3, 6, 7\}, \\ \pi_6 &= \{3, 5, 7\}, \\ \pi_7 &= \{3, 5, 6, 9\}, \\ \pi_8 &= \{9\}, \\ \pi_9 &= \{7, 8\}, \\ \pi_{10} &= \{11\}, \\ \pi_{11} &= \{10\}, \\ \pi_{12} &= \emptyset. \end{aligned}$$

EXAMPLE 6.3 (d -cells and Simplicial Complex). *In Figure 1, the d -cells (or the complete subgraphs with $d + 1$ nodes), for $d \in \{0, 1, 2, 3\}$ are*

$$\begin{aligned} C_0 &= V, \\ C_1 &= E, \\ C_2 &= \{\{2, 3, 4\}, \{3, 5, 6\}, \{3, 6, 7\}, \{3, 5, 7\}, \{5, 6, 7\}, \\ &\quad C_3 = \{\{3, 5, 6, 7\}\}. \end{aligned}$$

The simplicial complex is $C = \bigcup_{i=0}^3 C_i$.

EXAMPLE 6.4 (Node neighbourhood of a cell). *In Figure 1, $\pi_{\{12\}} = \emptyset = \pi_{\{2,3,4\}}$ and $\pi_3 = \{1, 2, 4, 5, 6\}$. Also, $\pi_{\{3,5,6\}} = \{7\}$.*

EXAMPLE 6.5 (Boundary of a cell). *The boundary of 0-cells is always an empty set. In Figure 1, the boundary of the 1-cell $\{7, 9\}$ is*

$$\partial(\{7, 9\}) = \{\{7\}, \{9\}\}.$$

The boundary of the 2-cell $\{2, 3, 4\}$ is

$$\partial(\{2, 3, 4\}) = \{\{2, 3\}, \{2, 4\}, \{3, 4\}\},$$

and the boundary of the 3-cell $\{3, 5, 6, 7\}$ is

$$\partial(\{3, 5, 6, 7\}) = \{\{3, 5, 6\}, \{3, 5, 7\}, \{3, 6, 7\}, \{5, 6, 7\}\}.$$

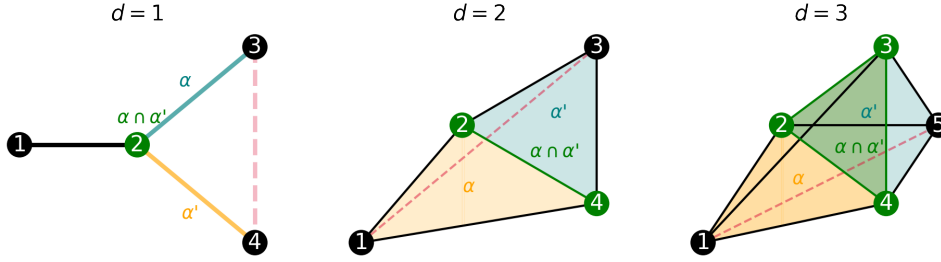


FIG. 6. Neighborhood condition depicted, for $d \in \{1, 2, 3\}$. For all dimensions, the neighbouring cells α and α' are drawn in blue and yellow, respectively, whilst the common boundary $(\alpha \cap \alpha')$ is represented in green. The presence (or absence) of the red dashed edge in the simplicial complex defines whether α and α' are transverse or parallel. In all cases, the intersection $\gamma := \alpha \cap \alpha'$ is a $(d-1)$ -cell such that $\gamma < \alpha, \alpha'$, which guarantees that for α and α' to be neighbours, it is sufficient to reach the cell neighbourhood condition 1. is reached. This result is a consequence of [Theorem 7.4](#).

EXAMPLE 6.6 (Cell neighborhood). In [Figure 1](#), the 0-cell $\{12\}$ has no neighbours, as well as the 1-cell $\{10, 11\}$, the 2-cell $\{2, 3, 4\}$ and the 3-cell $\{3, 5, 6, 7\}$. The 2-cell $\{3, 4\}$ has 6 neighbours, in which 2 are transverse ($\{2, 3\}, \{2, 4\}$) and 4 are parallel ($\{1, 3\}, \{3, 5\}, \{3, 6\}$ and $\{3, 7\}$). The 2-cell $\{3, 5, 7\}$ has 3 neighbours, $\{3, 6, 7\}, \{3, 5, 6\}$ and $\{5, 6, 7\}$, in which all of them are transverse.

EXAMPLE 6.7 (Cell Neighborhood condition). In [Figure 6](#), we have the characterization of neighborhood of d -cells, α (blue) and α' (yellow), for $d \in \{1, 2, 3\}$. Suppose that the red-dashed edge belongs to the graph. For $d = 1$, we have that $\alpha = \{2, 3\}$ and $\alpha' = \{2, 4\}$ are transverse neighbors, once that the 2-cell $\beta = \{2, 3, 4\}$ is such that $\beta > \alpha, \alpha'$. Analogously, for $d = 2$, the 2-cells $\alpha = \{1, 2, 4\}$ and $\alpha' = \{2, 3, 4\}$ are transverse once that $\beta = \{1, 2, 3, 4\}$ is a 3-cell such that $\beta > \alpha, \alpha'$. Also, for $d = 3$, $\alpha = \{1, 2, 3, 4\}$, $\alpha' = \{2, 3, 4, 5\}$ are transverse once that $\beta = \{1, 2, 3, 4, 5\}$ is a 4-cell such that $\beta > \alpha, \alpha'$. Regardless of the existence of the red-dashed edge in the graph, we have that, for $d \in \{1, 2, 3\}$, there is a $(d-1)$ -cell, $\gamma := \alpha \cap \alpha'$ such that $\gamma < \alpha, \alpha'$. This fact can be justified by the result of [Theorem 7.2](#), which guarantees that is sufficient to have a common boundary between two d -cells so they can be neighbours. The dashed-red edge's absence (or presence) guarantees they are parallel (transverse) neighbours.

EXAMPLE 6.8 (Forman-Ricci curvature). In [Figure 1](#), $F_1(\{3, 4\}) = 1 + 2 - 4 = -1$, $F_2(\{3, 5, 7\}) = 1 + 3 - 0 = 4$.

7. Demonstrations. Here we are considering π_α, π_x and the concepts of abstract simplicial complexes as defined in [section 2](#).

THEOREM 7.1. Let C_d be the set of all d -cells of a simplicial complex, as defined in [section 2](#). Then,

$$(7.1) \quad C_d = \left\{ \alpha := \{x_0, \dots, x_d\}, x_i \in \pi_{\alpha \setminus \{x_i\}}, \forall i \right\}.$$

Proof. First inclusion will be proven by contradiction. Let $\alpha \in C_d$. Suppose that α is not contained in the right-hand side of the equation above, *i.e.*, there exists $x \in \alpha$ such that $x \notin \pi_{\alpha \setminus \{x\}}$. It means that exists $y \in \alpha$ such that $y \neq x$ and $x \notin \pi_y$, which implies that α does not belong to C_d .

Also, let α as on the right-hand side in (7.1), from the definition of the set on the right-hand side, in G every pair of vertices in α is connected. Also $|\alpha| = d + 1$. Define $V_\alpha = \alpha$ and $E_\alpha = \{(x_i, x_j) \mid x_i, x_j \in V_\alpha, x_i \neq x_j\}$ such that $G_\alpha = (V_\alpha, E_\alpha)$. It is clear that G_α is a complete subgraph with $d + 1$ nodes and we can identify $V_\alpha \sim G_\alpha$. It follows that $\alpha \in C_d$. \square

THEOREM 7.2. *Let $\alpha, \alpha' \in C_d$, $\alpha \neq \alpha'$. They are neighbours if and only if $\alpha \cap \alpha'$ is the $(d - 1)$ -cell that is common to the boundaries of α and α' .*

Proof. The forward implication is proven as follows: Suppose condition 1. of the cell neighbourhood is satisfied. There exists $\gamma \in C_{d-1}$ such that $\gamma < \alpha, \alpha'$. In particular, $\gamma \subset \alpha, \alpha'$ and $|\gamma| = d$. It is sufficient to prove that $\gamma = \alpha \cap \alpha'$. The inclusion $\gamma \subseteq \alpha \cap \alpha'$ is obvious. Suppose, by absurdity, that there exists $x \in \alpha \cap \alpha'$ such that $x \notin \gamma$. Once the first inclusion is valid, it follows that $\gamma \cup \{x\} \subset (\alpha \cap \alpha') \cup \{x\} = \alpha \cap \alpha'$, which lead us to $|\gamma \cup \{x\}| \leq d$.

Now, suppose that condition 2. is reached. There exists $\beta \in C_{d+1}$ such that $\beta > \alpha, \alpha'$. In particular, $\beta \supset \alpha \cap \alpha' := \gamma$. First, we need to prove that $|\gamma| = d$. Note that we can write $\beta = \alpha \cup \{x\}$, for some $x \notin \alpha$. Analogously, we can write $\beta = \alpha' \cup \{y\}$, for some $y \notin \alpha'$, with $x \neq y$. By intersecting this equalities we have $\beta = (\alpha \cup \{x\}) \cap (\alpha' \cup \{y\}) = [\alpha \cap (\alpha' \cup \{y\})] \cup [\{x\} \cap (\alpha' \cup \{y\})] = [\gamma \cup (\alpha \cap \{y\})] \cup [(\{x\} \cap \alpha') \cup (\{x\} \cap \{y\})] = \gamma \cup \{x, y\}$. Thus, $|\gamma| = |\beta| - 2 = d$. Suppose that $\gamma \notin C_{d-1}$. Then, there exists $y \in \gamma$ such that $y \notin \bigcap_{\substack{x \in \gamma \\ x \neq y}} \pi_x$. However, $\gamma \subset \alpha$, and it would imply that $\alpha \notin C_d$. The opposite implication of the theorem is obvious. \square

THEOREM 7.3. *Let $\alpha, \alpha' \in C_d$. Then, α and α' are neighbours if and only if $|\alpha \cap \alpha'| = d$.*

Proof. It follows as a corollary from [Theorem 7.2](#). This neighbourhood condition can be better elucidated in [Example 6.7](#). \square

THEOREM 7.4. *Let $\alpha, \alpha' \in C_d$. Then, the neighborhood condition 2. implies the condition 1., i.e., α and α' are neighbours if and only if the condition 1. of cell neighbourhood is reach.*

Proof. It follows as a corollary from [Theorem 7.2](#). \square

THEOREM 7.5. *Let $\alpha \in C_d$, and N_α as defined originally in [section 3](#). Then,*

$$(7.2) \quad N_\alpha = \bigsqcup_{\gamma \in \partial(\alpha)} \bigcup_{\substack{x \in \pi_\gamma \neq \emptyset \\ x \notin \alpha}} \{\gamma \cup \{x\}\}.$$

Proof. Let $\alpha' \in N_\alpha$. From [Theorem 7.2](#), there exists $\gamma \in C_{d-1}$ such that $\gamma = \alpha \cap \alpha'$ and in particular, $|\gamma| = d$. Once that $|\alpha| = |\alpha'| = d + 1$ and $\gamma \subset \alpha, \alpha'$, there exists $x \in V \setminus \alpha$ such that we can write $\alpha' = \gamma \cup \{x\}$. Analogously, there exists $y \in V \setminus \alpha'$ such that we can write $\alpha = \gamma \cup \{y\}$. It is clear that $\pi_\gamma \setminus (\alpha \setminus \gamma) = \pi_\gamma \setminus \{y\}$. Suppose this set is not empty. We need to prove that $x \in \pi_\gamma \setminus (\alpha \setminus \gamma)$. By absurdity, suppose that x is not in this set. By using set complementary property, we have that $x \in (\pi_\gamma)^c \cup (\alpha \setminus \gamma)$. If $x \in \alpha \setminus \gamma$, then $\alpha = \alpha'$. If $x \in \pi_\gamma^c$, then there exists $z \in \gamma$ such that $x \notin \pi_\gamma$, which implies that α' is not a d -cell.

The opposite inclusion is proven as follows: Let α' be such that $\alpha' = \gamma \cup \{x\}$, for some $x \in \pi_\gamma \setminus (\alpha \setminus \gamma)$, and some $\gamma \in \partial(\alpha)$. Note that $|\alpha \cap \alpha'| = |\alpha \cap (\gamma \cup \{x\})| = |(\alpha \cap \gamma) \cup (\alpha \cap \{x\})| = |\gamma| = d$. The result follows from applying [Theorem 7.2](#) once proven that $\alpha' \in C_d$. Indeed, $|\alpha'| = |\gamma \cup \{x\}| = d + 1$. Suppose by absurdity that $\alpha' \notin C_d$. Then, by using the the result of [Theorem 7.1](#), there exists $z \in \alpha'$ such that

$z \notin \pi_{\alpha' \setminus \{z\}}$. In case of $z = x$, we have that it contradicts that $x \in \pi_\gamma \setminus \{y\}$. Also, if $z \neq x$, we would have that $z \in \gamma$ and it contradicts that $\alpha \in C_d$. \square

THEOREM 7.6. *Let $\alpha \in C_d$, $\gamma \in \partial(\alpha)$ and $x \in \pi_\gamma$, $x \notin \alpha$. Let $\alpha' := \gamma \cap \{x\}$. Then, $\alpha \in T_\alpha$ if and only if $x \in \pi_\alpha$.*

Proof. Note that **Theorem 7.2** and **Theorem 7.5** guarantees that $\alpha' \in N_\alpha$ and that $\gamma = \alpha \cap \alpha'$. Having said that, consider $\beta := \alpha \cup \alpha' = \gamma \cup \{x, y\}$, for some $y \notin \alpha$, $y \neq x$. If $x \in \pi_\alpha$, then $\beta \in C_{d+1}$, and $\beta > \alpha, \alpha'$. Otherwise, there exists $x_0 \in \alpha$ such that $x \notin \pi_{x_0}$ and then $\beta \notin C_{d+1}$. \square

THEOREM 7.7. *Let $\alpha \in C_d$ and T_α as described in [section 3](#). Then,*

$$(7.3) \quad T_\alpha = \bigsqcup_{\gamma \in \partial(\alpha)} \bigcup_{\substack{x \in \pi_\gamma \neq \emptyset \\ x \in \pi_\alpha \neq \emptyset \\ x \notin \alpha}} \{\gamma \cup \{x\}\}.$$

Proof. It follows as a corollary from **Theorem 7.6** and the characterization of the neighbourhood of α in **Theorem 7.5**.

THEOREM 7.8. *Let P_α as defined in [section 3](#). Then,*

$$(7.4) \quad P_\alpha = \bigsqcup_{\gamma \in \partial(\alpha)} \bigcup_{\substack{x \in \pi_\gamma \neq \emptyset \\ x \notin \pi_\alpha \neq \emptyset \\ x \notin \alpha}} \{\gamma \cup \{x\}\}.$$

Proof. It also follows as a corollary from **Theorem 7.6** and the characterization of **Theorem 7.5**. \square

THEOREM 7.9. *Let H_α as defined in [section 3](#). Then,*

$$(7.5) \quad H_\alpha = \bigcup_{x \in \pi_\alpha \neq \emptyset} \{\alpha \cup \{x\}\}.$$

Proof. Let $\beta \in H_\alpha$. In particular, $\beta \supset \alpha$ implies that exists $x \notin \alpha$ such that we can write $\beta = \alpha \cup \{x\}$. It is clear that $x \in \pi_\alpha$, otherwise β would not be a $(d+1)$ -cell. Let β in be a set of the form $\beta = \alpha \cup \{x\}$, for some $x \in \pi_\alpha$. It is enough to show that $\beta \in C_{d+1}$, which is immediate, once that $|\beta| = d+2$. \square

THEOREM 7.10. *Let $\alpha \in C_d$. Then,*

$$(7.6) \quad |T_\alpha| = (d+1) |H_\alpha|.$$

Proof. Note that $\pi_\alpha = \pi_\gamma \cap \pi_{\alpha \setminus \gamma}$, for all $\gamma \in \partial(\alpha)$. Thus, by taking the cardinality of T_α and H_α using the equalities in **Theorem 7.7** and **Theorem 7.9**, we have

$$(7.7) \quad |T_\alpha| = \sum_{\gamma \in \partial(\alpha)} |\pi_\alpha| = (d+1) |\pi_\alpha| = (d+1) |H_\alpha|. \quad \square$$

THEOREM 7.11. *Let $G = (V, E)$. For all $d \geq 1$ and $\alpha \in C_d$, the FRC is bounded by*

$$(7.8) \quad 2 \cdot (d+1) - |V| \leq F_d(\alpha) \leq |V|$$

Proof. From (3.1) and (3.2), it is clear that we have that the minima of F_d are reached when all neighbours of α are parallel. Analogously, the maxima are reached when all neighbours of α are transverse. Also, the maximum number of neighbours of a d -cell is $|V| - (d + 1)$. It follows that the minima is $2 \cdot (d + 1) - |V|$ and the maxima is $|V|$. \square